Equilibration and Exchange of Fluorescently Labeled Molecules in Skinned Skeletal Muscle Fibers Visualized by Confocal Microscopy

T. Kraft,*‡ M. Messerli,§ B. Rothen-Rutishauser,§ J.-C. Perriard,§ T. Wallimann,§ and B. Brenner‡
‡Department of Clinical Physiology, Medical School of Hannover, D-30627 Hannover, Germany; and §Institute of Cell Biology, ETH-Hönggerberg, CH-8093 Zürich, Switzerland

ABSTRACT Confocal laser fluorescence microscopy was used to study in real time under nearly physiological conditions the equilibration and exchange characteristics of several different fluorescently labeled molecules into chemically skinned, unfixed skeletal muscle fibers of rabbit psoas. The time required for equilibration was found to vary widely from a few minutes up to several days. Specific interactions of molecules with myofibrillar structures seem to slow down equilibration significantly. Time for equilibration, therefore, cannot simply be predicted from diffusion parameters in solution. Specific interactions resulted in characteristic labeling patterns for molecules like creatine kinase (muscle type), pyruvate kinase, actin-binding IgG, and others. For the very slowly equilibrating Rh-NEM-S1, changes in affinity upon binding to actin in the absence of calcium and subsequent slow cooperative activation, beginning at the free end of the filament at the H-zone, were observed. In the presence of calcium, however, binding of Rh-NEM-S1 was homogeneous along the whole actin filament from the very beginning of equilibration. The dissociation properties of the dynamic interactions were analyzed using a chase protocol. Even molecules that bind with rather high affinity and that can be removed only by applying extreme experimental conditions like Rh-phalloidine or Rh-troponin could be displaced easily by unlabeled homologous molecules.

INTRODUCTION

The movement of molecules through the cytoplasm of cells has been a topic of many investigations. Apparently, it is quite different from diffusion in solution and depends strongly on the structure and viscosity of the cellular compartment. This holds true even for very small molecules, e.g., diffusion of cGMP in rod outer segments of the retina (Olson and Pugh, 1993) or calcium in muscle (Engel et al., 1994). Evidence from several laboratories using different experimental methods points to the fact that even the cytoplasm of "less complex cells" like oocytes is dominated by a highly organized cytoskeleton (Horowitz and Moore, 1974). Most of these ordered cytoskeletal elements control cell shape and cell mobility and are involved in intracellular transport. Particularly, the function of striated (and other) muscle cells is based on a highly organized contractile apparatus consisting of sarcomeric myofibrils. In fact, there is very limited space for free diffusion in these cells: 50–80% of the cell volume, depending on the muscle type, is filled by the contractile apparatus, and up to 30% may be occupied by mitochondria (Jones and Round, 1990). There is also evidence that the cytosolic enzymes, which supply energy for movement and transport, are not distributed uniformly over the whole cytoplasm but are located in distinct areas of the cell (Wegmann et al., 1992; Saks and Ventura-Clapier, 1992), leading to the idea of a close coupling between localization and function of many cytomatrix components. In addition, the so called cytoplasmic systems, among them the glycolytic enzymes, are organized in large multienzyme complexes (Kurganov et al., 1985) functioning as metabolic systems (Keleti, 1990). This complex organization of the cytosol as well as the cytomatrix of cells and possible intermolecular interactions have to be taken into account when analyzing the movement of molecules inside cells.

Experimentally, the diffusion of extrinsic proteins or other molecules into native, permeabilized, or fixed cells is a standard method not only for the identification and localization of their subcellular binding sites, but also for studying the physiological effects of such compounds on cellular parameters, e.g., cell division, motility and metabolic regulation. In the past, various approaches have been used to study the movement of small and large probes through different cells. Radioactively labeled molecules were used to measure diffusion through oocytes, axons or muscle fibers (Horowitz and Moore, 1974; Paine et al., 1975; Kushmerick and Podolsky 1969). Fluorescence recovery after photobleaching is a method for analyzing diffusion of fluorescently labeled probes injected into the cytoplasm of cells (Edidin et al., 1976; Wojcieszyn et al., 1981). Maughan and Lord (1988) used microvolumetric sampling methods to analyze protein diffusivities in skinned frog skeletal muscle

Received for publication 13 January 1995 and in final form 20 July 1995.

Address reprint requests to Dr. Theresia Kraft, National Institutes of Health, NIAMS, Bldg. 6, Room 114, 9000 Rockville Pike, Bethesda, MD 20892. Tel.: 301-496-5417; Fax: 301-402-0009; E-mail: te1@helix.nih.gov.

Dr. Kraft's present address: National Institutes of Health, NIAMS, Bethesda, MD 20892.

Abbreviations used: Rh-PK, rhodamine-labeled pyruvate kinase; TRITC-anti-actin-IgG, TRITC-labeled actin-specific antibody; TxR-DaM-IgG, Texas-Red-conjugated donkey anti-mouse IgG; Rh-NEM-S1, rhodamine-labeled, *N*-ethylmaleimide-modified myosin-subfragment 1; Rh-Cald., Rhodamine-labeled intact caldesmon; Rh-MM-CK, rhodamine-labeled muscle-type creatine kinase (dimer); Rh-BB-CK, rhodamine-labeled brain-type creatine kinase (dimer); Rh-F_{ab}(1–7), rhodamine-labeled antibody binding to the first seven N-terminal residues of actin.

0006-3495/95/10/1246/13 $2.00

fibers. Recently, the diffusibility of gene products directed by a single nucleus in the cytoplasma of multinucleated muscle fibers was studied using molecular biology techniques and was shown to be quite limited spatially in muscle (Ono et al., 1994). Confocal microscopy (Minsky, 1957; Sheppard, 1987) is another microscopical technique that allows to study the movement and final distribution of fluorescently labeled probes in different cells with very high resolution.

The diffusion of proteins or fragments thereof into skinned muscle fibers or the exchange of intrinsic fiber proteins by modified equivalents in order to influence mechanical and structural parameters, such as isometric force generation and changes in x-ray reflections, is a widely used method. Before analyzing such effects, one has to quantitate diffusion of the compound in question and to ensure that distribution within the cell has reached equilibrium. However, little is known about diffusion characteristics of such molecules within the fibers, i.e. pathways, exchange, and interaction with endogenous proteins or with subsarcomeric structures. For muscle, it has generally been assumed that diffusion of the proteins and enzymes used is fast, such that they equilibrate within several minutes inside a skinned muscle fiber.

In our present work, we used confocal microscopy to study the equilibration and its limiting factors of several fluorescently labeled muscle- and non-muscle proteins, as well as smaller fluorescent compounds in demembranated, unfixed rabbit skeletal muscle fibers. By using confocal laser fluorescence microscopy, it was possible to follow directly and in real time the equilibration of labeled molecules in muscle fibers under physiological conditions. In addition, the reversibility of this process and also the exchange between endogenous protein and externally added protein could be studied. A preliminary account of this work has been presented earlier (Kraft et al., 1993).

MATERIALS AND METHODS

Fluorescently labeled molecules

Rh-phalloidine, rhodamine 123, MM-CK, BB-CK and pyruvate-kinase were obtained from Sigma. FITC- and Texas-Red labeled antibodies were from Cappel, Dynatech, Zürich, Switzerland.

Myosin-subfragment 1 (S1) was prepared according to the method of Weeds and Taylor (1975). A1-S1 was purified using DEAE-Sephacel ion-exchange chromatography. *N*-ethylmaleimide-modified myosin-subfragment 1 (NEM-S1) was prepared as described by Williams et al. (1984). The procedure was modified with respect to time and temperature of the reaction of S1 with N-ethylmaleimide (Schnekenbühl et al., 1992).

Rh-NEM-S1, Rh-caldesmon (intact), Rh-pyruvate kinase, Rh-troponin and Rh-creatine kinase from muscle (Rh-MM-CK) and from brain (Rh-BB-CK) were obtained by modifying the proteins with rhodamine-X iodoacetamide (Molecular Probes, Inc.). TRITC-F_{ab}(1–7) anti actin antibody fragment (DasGupta and Reisler, 1992) and TRITC-anti actin IgG (Sigma A 1804) were obtained by modifying the proteins with tetramethylrhodamine isothiocyanate (Sigma). Subsequently the excess rhodamine-X iodoacetamide or the excess TRITC, respectively, were removed by gel filtration (Sephadex G-25, Pharmacia). The elution buffer contained 10 mM imidazole, 2 mM $MgCl_2$, 1 mM EGTA, 1 mM DTT and 34 mM K-propionate. At least two purification runs were found to be necessary to reduce unbound rhodamine-X iodoacetamide or TRITC below levels that were detected by confocal fluorescence microscopy.

Rh-caldesmon was kindly provided by Dr. J.M. Chalovich, ECU, NC, U.S.A., the TRITC-F_{ab}(1–7) antibody fragment by Dr. E. Reisler, UCLA, U.S.A. The polyclonal goat antibody against chicken M-band protein preparation containing 165 kDa M-protein as well as 185 kDa myomesin (Eppenberger et al., 1981; Grove et al., 1984) was generated by standard procedures at the Institute of Cell Biology, ETH Zürich, Switzerland.

For some molecules the effect of the rhodamine-labeling on their physiological/biochemical properties was studied. We found no difference in the effects of Rh-NEM-S1, Rh-caldesmon, Rh-troponin and TRITC-F_{ab}(1–7) on the mechanical properties of skinned muscle fibers as well as on their behavior in solution studies compared to the unlabeled proteins.

Solutions

For diffusion of fluorescent components into the fibers the respective fluorescently labeled molecules were immersed in relaxing solution. This solution contained 10 mM imidazole, 2 mM $MgCl_2$, 3 mM EGTA, 2 mM MgATP or alternatively 2 mM MgATPγS, 30 mM glutathion, 0.2 mM Ap_5A, 200 mM glucose (and 0.5 units/ml hexokinase for solutions with MgATPγS); the ionic strength was adjusted to 120 mM by adding K-propionate; pCa was 8.0 (except when Rh-NEM-S1 was diffused into a fiber in the presence of ATPγS at pCa 4.5). All solutions were adjusted to pH 7.0 at the experimental temperature of 5°C or at 22°C for real time confocal microscopy.

Preincubation of muscle fibers with Rh-NEM-S1 occurred in relaxing solution containing MgATPγS, for all other preincubations and diffusion experiments we used the relaxing solution containing MgATP. For washing out unbound fluorescently labeled molecules, we used the same relaxing solution but without adding the tested molecules.

Fiber preparation and mounting

Small bundles from rabbit psoas muscle were prepared and chemically skinned with Triton-X-100 according to a method described earlier (Brenner, 1983; Yu and Brenner, 1989). Single fibers, isolated from these bundles, were stored for up to five days in skinning solution containing protease inhibitors (Kraft et al., 1995). For some of the experiments we used not only single fibers that were freshly isolated but also fibers from bundles that had been stored in liquid nitrogen for some time. In order to store the bundles in liquid nitrogen without any detectable structural damage, we added sucrose as cryo-protectant to the solution. In short, before freezing, after skinning in Triton-X-100, the bundles were successively incubated for at least 30 minutes each in skinning solution containing 0.5 M, 1.0 M, 1.5 M and 2 M sucrose (Mallinckrodt). After equilibration with 2 M sucrose, the bundles were cut into sections of about 1–2 cm in length and rapidly frozen in liquid propane. From there, the bundles were quickly transferred into liquid nitrogen for long term storage. For thawing, the bundles were transferred directly from liquid nitrogen into skinning solution containing 2 M sucrose. Subsequently, the bundles were again incubated successively for 30 minutes each in skinning solution with 1.5 M, 1 M, 0.5 M sucrose and finally kept in normal skinning solution. From these bundles, single fibers were isolated as usual. Several studies using x-ray diffraction and mechanical methods were carried out to demonstrate that none of the parameters tested (e.g., equatorial intensities, isometric force, shortening velocity, fiber ATPase activity, and fiber stiffness under various conditions) revealed any changes due to the freezing procedure (details will be published elsewhere). Regarding the results presented in this paper, fibers isolated after freezing and thawing did not show any differences in the parameters tested compared with fibers that had been freshly isolated.

In the present study, for all real time equilibration and exchange experiments, unfixed skinned fibers were used. For confocal microscopy, the fibers were mounted in a flat, home-made, flow-through chamber on a

microscopic slide. The chamber, ~200 μM deep, was closed with a coverslip so that the fibers were completely surrounded by solution. For adding the fluorescently labeled proteins, new solution could be sucked through the chamber while the fiber remained in place on the microscope stage.

When following the time course of equilibration and exchange, no reagents were added to reduce photobleaching. The observation time at each time point was short (<20 s), and the intensity of the exciting light was kept as low as possible. In between the different scans, the fibers were kept in the dark so that even after several days of incubation fluorescence intensity was not reduced. If scanning occurred somewhat more frequently over a longer time period, e.g., in exchange experiments, images were taken also at neighboring spots to ensure that the decrease in intensity was not due to photobleaching. In some cases, when it was necessary to ensure that no further changes in intensity ratio occurred at very late time points (e.g., Rh-NEM-S1, Fig. 7), *after* the desired time of incubation the fibers were rinsed briefly in solution without the fluorescently labeled molecules for reducing the background intensity and then were fixed in relaxing solution containing 0.2% glutaraldehyde and 2% *p*-formaldehyde. These fibers were then mounted on a microscopic slide in anti-bleaching mounting medium containing 70% glycerol, 30 mM Tris-HCl, pH 9.5, and 5% (w/v) *n*-propyl gallate.

Confocal microscopy and analysis of equilibration time

The laser confocal system consisted of a Zeiss Axiophot fluorescence microscope, a Bio-Rad MRC-600 confocal scanner unit, and a Silicon Graphics Personal Iris 4D/25 workstation with 32 Mbytes of main memory (Silicon Graphics, Mountain View, CA). The images were recorded with oil immersion objectives using a Zeiss Neofluar 40×/1.3 objective, a Zeiss 63×/1.4 objective, or a Zeiss Plan Apochromat objective 40×/1.0 with a working distance of 0.31 mm. The system was equipped with an argon/krypton mixed gas laser. Image processing was done on the Silicon Graphics workstation using "Imaris" (Messerli et al., 1993), a three-dimensional multichannel image-processing software specialized for confocal microscopic images (Bitplane AG, Technopark, Zürich, Switzerland).

We used this system to follow the time course of equilibration of fluorescently labeled molecules over the cross section of the fibers as well as the equilibration in longitudinal direction in the different parts of the sarcomeres. Initially, from series of optical sections, three-dimensional images of the fibers were reconstructed to analyze the intensity distribution within the whole observed fiber section in three dimensions. Fig. 1 shows a fiber cross section that was reconstructed from 80 longitudinal optical sections and a longitudinal section through the core of the same muscle fiber that had been equilibrated with 1.7 μM Rh-phalloidine. Analysis of such reconstructed images showed some indication of absorbance in thick specimens, i.e., lower intensity at the bottom part of the fiber in Fig. 1. This was derived from the fact that after equilibration is essentially complete, fibers should have the same density of fluorescently labeled molecules at the "proximal" and at the "distal" end of the fibers as viewed along the optical axis. The differences in detected fluorescence intensity between proximal and distal areas were attributed to the attenuation of both, exciting and emitted light due to absorbance of the light on its way through the specimen. However, as shown in Fig. 1, the attenuation of intensity in the layers toward the bottom of the fiber after complete equilibration, in fact, was rather limited (<50%) for all fluorescently labeled molecules at the concentration (~1.7 μM) used in this study. Nevertheless, because such attenuation can cause an apparent inhomogeneity of fluorescent labeling that is not due to incomplete equilibration, we had to account for this effect in our analysis.

Using three-dimensional reconstruction from series of optical sections with correction of absorbance effects, however, appeared to be impractical for following the time course of equilibration because the recording of one complete data set for a three-dimensional reconstruction takes some 20–30 min, depending on the number of optical sections. For molecules that equilibrate within several minutes or a few hours, the distribution of fluorescently labeled molecules would change significantly even while recording sections for a single reconstruction. Additionally, recording of several series of optical sections could cause artifacts due to photobleaching during scanning. Alternatively equilibration, in principle, could be followed by recording optical sections in the z direction through the fibers without using three-dimensional reconstruction. However, such z sections do not provide information about the axial intensity distribution within each sarcomere, which was found to be another essential criterion for equilibration. For example, for Rh-NEM-S1 equilibrium is reached only when the intensity distribution within each sarcomere is identical over the entire fiber (cf. Fig. 7 below) because Rh-NEM-S1 does not bind to the whole actin filament at once (Fig. 6).

Therefore, instead of using three-dimensional reconstruction of cross sections, a simplified procedure was used to follow the time course of equilibration and exchange of the molecules in real time. We recorded a time series of single longitudinal optical sections through the core-region of the unfixed fibers. From these sections, intensity profiles across the fibers were obtained. To avoid artifacts possibly caused by attenuation of intensity due to shape and thickness of the specimen, absolute intensities were *not* used to determine time for equilibration but, instead, the ratio of the fluorescence intensity ($I_{\text{core}}/I_{\text{outer layers}}$) was determined as a function of

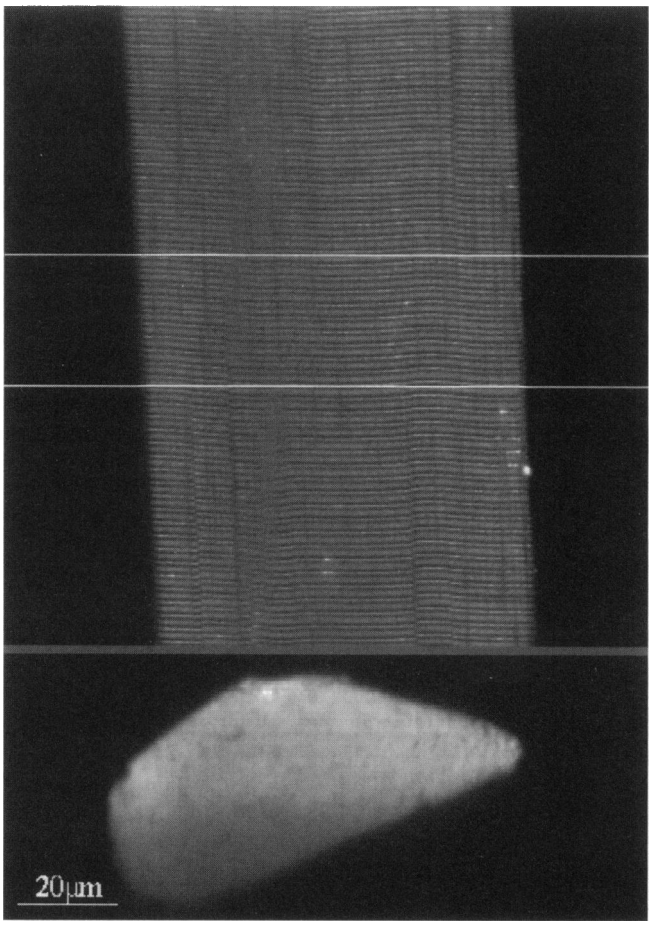

FIGURE 1 Longitudinal optical section through the core (above) and cross section (below) through a muscle fiber labeled with 1.7 μM Rh-phalloidine (time allowed for equilibration was 2 h). The cross section was reconstructed from a series of 80 longitudinal optical sections that were obtained with a Zeiss Plan Apochromat oil immersion 40×/1.0 objective. Setting of the neutral density filter was 1, and the distance between subsequent sections was 0.8 μm. To obtain this image, a longitudinal region of ~10 sarcomeres was averaged in each optical section as indicated by white horizontal lines in the top image.

time. From these intensity ratios, we took the time, after which no further changes of the intensity ratio above noise was detectable and no further changes in distribution of fluorescence along the sarcomeres could be seen, as the time range when equilibrium was reached.

In Fig. 2 the time course of equilibration is shown for Rh-F_{ab}(1–7), an antibody fragment directed against the first seven N-terminal residues of actin. Usually, the first series of images was started 30 s after adding the fluorescently labeled molecules; the time interval between successive images was 30 s. Subsequently, images were taken after longer time intervals (from several minutes to several hours, Fig. 2), depending on the overall time required to ensure that no further changes in intensity distribution occurred. To achieve sufficient spatial resolution, each image was the average of six scans completed in ~15 s.

The observed equilibration times (Fig. 3) were normalized with respect to the square of the fiber diameter, based on simple diffusion into a cylinder (Hill, 1948). The fiber diameter was measured from the longitudinal sections through the core region of the fiber. Such normalization, however, can only be an approximation because the fibers are usually not cylindrical and other factors than simple diffusion can dominate the time course of equilibration. Nevertheless, because the results with the different molecules show time courses that differ so greatly, a more detailed analysis of the results is very unlikely to lead to changes in the overall conclusion.

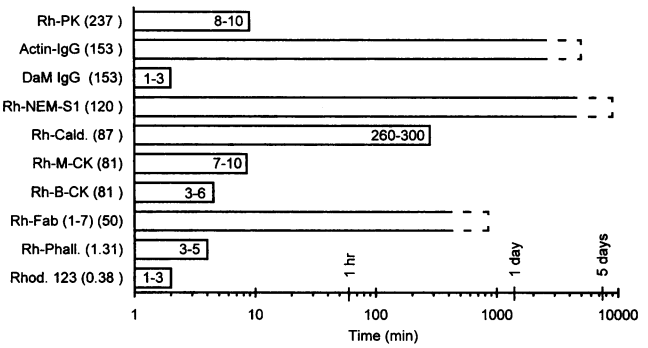

FIGURE 3 Time to reach homogeneous distribution throughout the fibers (equilibration time) for molecules of different molecular weights. Equilibration times observed in real time by confocal microscopy (T = 22°C). For all molecules, concentration was ~1.7 μM, the equilibration time was determined from the fluorescence intensity in longitudinal two-dimensional sections through the core of the fibers recorded at different points in time. Time for equilibration is normalized to the square of the fiber diameter. Numbers in each column are the equilibration times in minutes, and broken lines at the end of some columns illustrate uncertainty due to limited number of "snapshots" taken.

RESULTS

Time course of equilibration

To study parameters that influence the rate of equilibration of different molecules in chemically skinned but unfixed skeletal muscle fibers, we first followed the equilibration of several compounds with various molecular weights. The diagram in Fig. 3 summarizes the time required to reach homogeneous distribution of fluorescence throughout the whole fiber for compounds of molecular weights ranging from 0.38 up to 237 kDa. We used identical concentrations (1.7 μM) of fluorescently labeled molecules and followed the distribution of fluorescence intensity in the core of the fibers. Special attention was paid to maintain equal experimental conditions like the composition of solution, temperature, and flow, except for Rh-NEM-S1 MgATP was replaced by MgATPγS to avoid active force generation due to binding of Rh-NEM-S1 to actin. We determined the time from the first appearance of the fluorescently labeled molecules in the outermost layers of the fiber until no further changes in the ratio of fluorescence intensity in the core of the fiber versus the outer layers could be detected. The results are shown in Fig. 3, normalized for the square of the diameter of the fibers. For all molecules studied, the intensity ratio was close to unity when equilibrium was reached. This indicates that attenuation effects of intensity due to the thickness of the fibers were not relevant. It should be noted that in our experiments, because of the time span needed for the exchange of the solutions bathing the fibers (dead time), the time resolution was not high enough to determine equilibration times shorter than 2–3 min. Therefore, we could not distinguish between the effects of molecular weight on mobility of very fast equilibrating compounds such as Rh-123 (M_r 0.38 kDa) and the TxR-DaM-IgG (a Texas-Red-labeled donkey IgG against mouse, M_r 153 kDa). The data, however, show that for equilibration times longer than 2–3 min the time to reach homogeneous distribution is not simply a function of molecular weight.

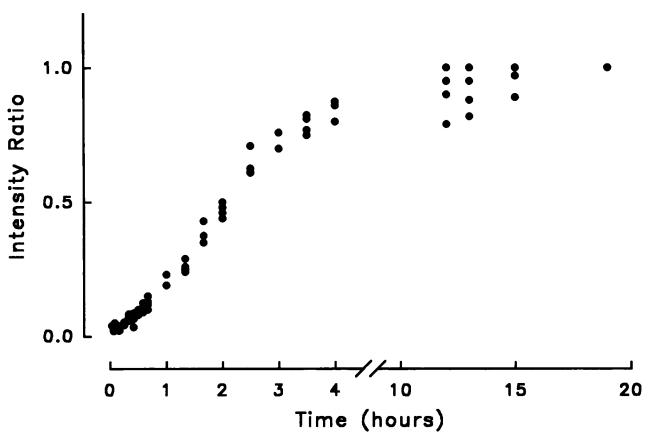

FIGURE 2 Time course of equilibration of a muscle fiber with 1.7 μM Rh-F_{ab}(1–7). The intensity ratio was determined from longitudinal optical two-dimensional sections through the core of the fiber as the ratio of the intensity in the core of the fiber over the intensity in the outermost layers. (Diameter of the fiber in the observed region was ~103 μm).

TxR-DaM-IgG, for which no specific binding sites inside the fiber are expected (Fig. 4 *A*), equilibrated within ~3 min. After equilibration was complete, fluorescence intensity inside the fiber, however, was only little higher than the intensity outside the fiber (Fig. 4 *A*). Nevertheless, a very weak sarcomeric pattern could be detected, indicating some low affinity binding to certain sarcomeric proteins.

In contrast, TRITC-anti-actin-IgG, which has the same molecular weight and shape as the TxR-DaM-IgG, but which binds specifically to actin (Fig. 4 *B*), needed more than 3 days for full equilibration. Furthermore, after equilibration the fluorescence intensity of TRITC-anti-actin-IgG

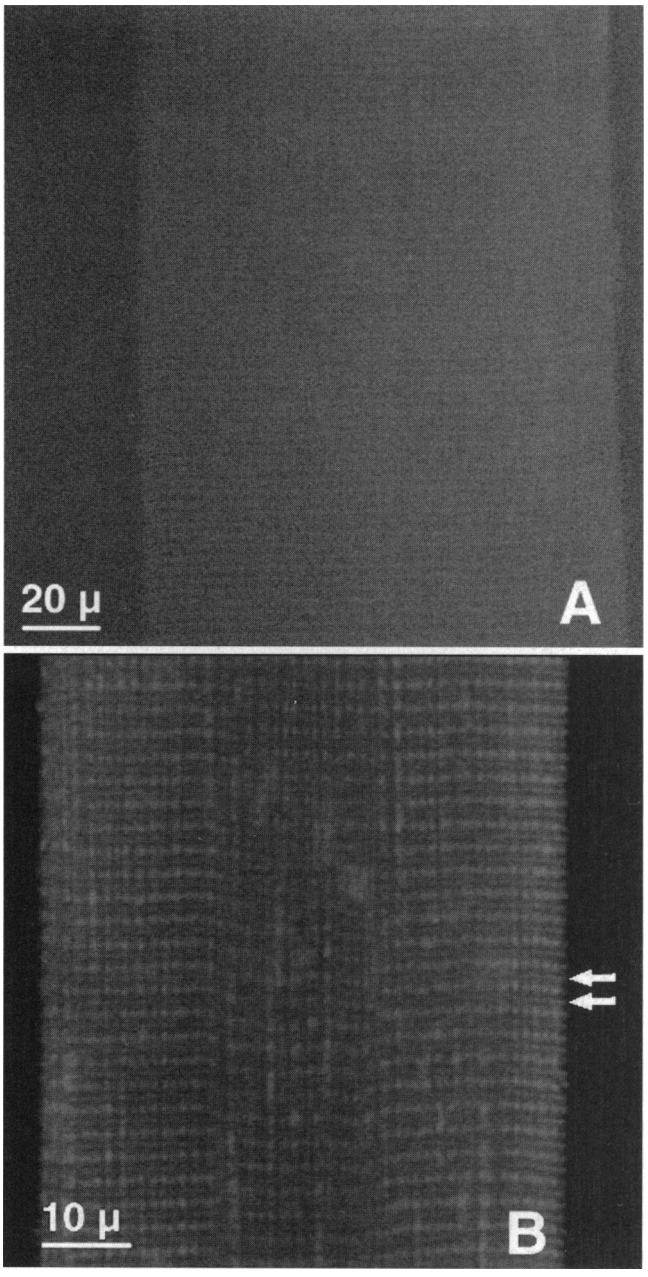

FIGURE 4 Confocal images of longitudinal optical sections through the core of unfixed skeletal muscle fibers. (*A*) incubated for 30 min with the non-muscle-specific Texas-Red-conjugated antibody DaM (TxR-DaM-IgG), and (*B*) after 48 h of incubation with TRITC-anti-actin-IgG. Arrows indicate H-zone. Equilibration of TRITC-anti-actin-IgG seems still incomplete because there is fluorescence intensity gradient from surface to core of fiber. TRITC-anti-actin-IgG appears to bind preferentially to actin filaments in the I-band of the sarcomeres. There is not much labeling in region of overlap between thin and thick filaments. Because specific binding of the antibody to actin, maximum fluorescence intensity inside fiber after equilibration is much higher than in the surrounding solution. Note that gain setting in *B* is lower than in *A* to avoid saturation of the photomultiplier. Therefore, background in *B* appears dark.

inside the fiber was much higher than in the periphery of the fiber.

TRITC-F_{ab}(1–7) (Fig. 5 *A*), a TRITC-labeled 50-kDa F_{ab} fragment of an antibody directed against the first seven N-terminal amino acid residues of actin (DasGupta and Reisler, 1992), took only ~12–14 h to reach homogeneous distribution (Fig. 2). Because of its high affinity binding to actin, after equilibration the fluorescence intensity inside the fiber again was very high.

Slow equilibration in the range of hours or days (Fig. 3) was also found for other proteins and substances that bind to fiber proteins, such as rhodamine-labeled caldesmon and Rh-NEM-S1 (Fig. 6). Fast equilibration in the range of 3–6 min, in our experiments perhaps limited by the dead-time of the solution exchange, was typical for Rh-brain-creatine-kinase (Rh-BB-CK, Fig. 5 *D*), which showed no high affinity binding inside the fiber.

In contrast to the effects of binding on the equilibration for large molecules like TRITC-anti-actin-IgG or TxR-DaM-IgG, we found that time for equilibration for the small molecules, e.g., Rh-123 and Rh-phalloidine, was not very different, although Rh-phalloidine also did bind with high affinity to actin filaments (data not shown). As a result of the specific binding of Rh-phalloidine to actin, the fluorescence intensity inside the fiber after equilibration was very high (comparable with the fluorescence intensity of TRITC-F_{ab}(1–7) shown in Fig. 5 *A*). The equilibration of Rh-phalloidine is expected to be slowed down because of the time required for saturation of the binding sites. It is possible, however, that equilibration of small molecules such as Rh-123 is faster than the time resolution such that we could not resolve the real difference between Rh-123 (no specific binding) and Rh-phalloidine with our approach. A slightly higher fluorescence intensity compared with the background fluorescence in the surrounding solution was also detectable for Rh-123, similar to what is shown for the nonspecific TxR-DaM-IgG in Fig. 4 *A*. However, Rh-123, which is normally accumulated into mitochondria of living cells, did not bind significantly to any sarcomeric protein in skinned muscle fibers. This is not surprising because in skinned fibers most mitochondria are damaged or lost and cannot accumulate the dye. The very weak sarcomeric pattern, visible after diffusion of Rh-123, might reflect either the available space for the fluorescently labeled compound or some low affinity, nonspecific binding to sarcomeric structures.

The data indicate that equilibration of molecules within unfixed skinned muscle fibers in general is slowed down dramatically by binding of the molecules to cytomatrix proteins, although other factors apparently also contribute to the large variability in time required for equilibration.

Spatial distribution of fluorescent labeling

The high spatial resolution of confocal microscopy allows identification of different sarcomeric structures like the H-zone, the A-band, the actomyosin overlap zone, the I-band, etc. Specific binding of the molecules to certain structures is expected to cause an increase in fluorescence intensity in the respective region within each sarcomere, resulting in a

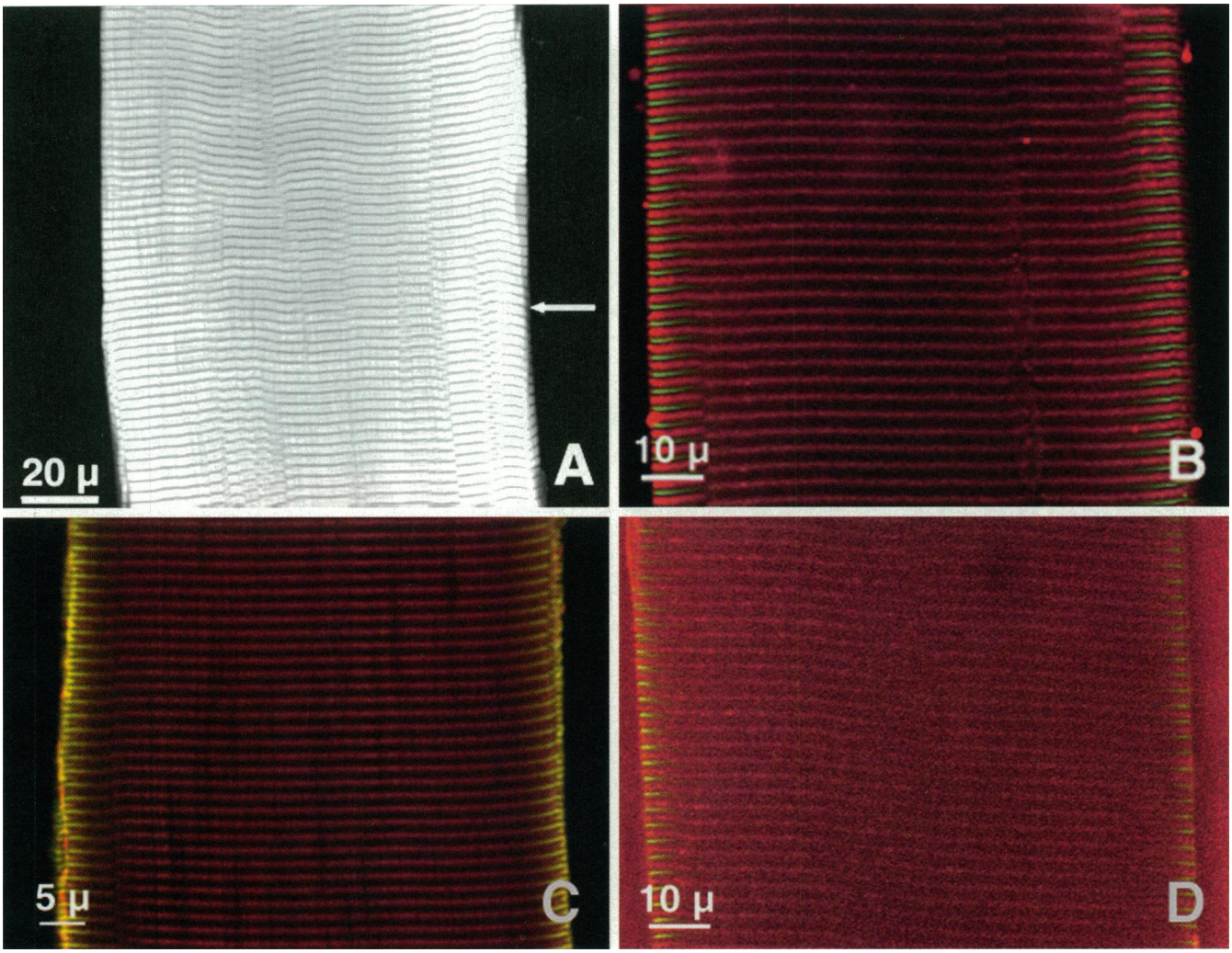

FIGURE 5 Confocal images of longitudinal optical sections through the core of unfixed fibers after equilibration with (*A*) TRITC-F_{ab}-antibody-fragment against the actin-residues (1–7) (F_{ab}(1–7), *arrow* marks the H-zone of a sarcomere), (*B*) Rh-pyruvate kinase, (*C*) Rh-creatine kinase from muscle (Rh-MM-CK), and (*D*) Rh-creatine kinase from brain (Rh-BB-CK). Image of Rh-BB-CK (*D*) was taken before washing. The solution still contained the fluorescent Rh-BB-CK molecules to demonstrate the small difference in intensity inside, caused by very weak binding of BB-CK to the I-band, versus the periphery of the fiber. This fluorescence is completely removed after a short wash, indicating very weak interaction of BB-CK with myofibrils. The fibers in *B-D* were preincubated with an antibody to the M-line-specific protein myomesin for at least 2 h, which was stained with a second, FITC-labeled antibody for ~4 h.

characteristic binding pattern. Furthermore, the time course of specific fluorescent labeling within each sarcomere can be analyzed. If equilibration time of some molecules in fact depends on their specific interaction with muscle fiber proteins, one would expect such binding to occur with significant affinity. The specific binding pattern should develop quite fast near the fiber surface but progress only slowly toward the core of the fiber.

To identify unambigously the different regions of each sarcomere, we used an antibody against the M-line protein myomesin as described in Fig. 5 *B* as a standard marker for the sarcomeric M-line.

Spatial distribution after equilibration

Actin-binding molecules. After equilibration, the rhodamine-labeled F_{ab} fragments of an antibody against the N-terminal amino acid residues 1–7 of actin (TRITC-F_{ab}(1–7), Fig. 5 *A*) as well as Rh-NEM-S1 (Fig. 7) were found to be distributed homogeneously all along the actin filaments without any preference for certain segments of the thin filament. The TRITC-anti-actin-IgG (Fig. 4 *B*), however, seemed to bind preferably to the actin filaments outside the region of overlap between thin and thick filaments.

Proteins located in the H-zone of the sarcomere. As mentioned previously, an antibody against the M-line proteins myomesin and M-protein (Eppenberger et al., 1981; Grove et al., 1984) was used as a marker for the M-line. It was detected with a secondary, FITC-labeled antibody (RaG). Fig. 5 *B* demonstrates its specific binding pattern within the sarcomeres, although only the outermost layers of the fiber were labeled and no complete equilibration was achieved within time of incubation (2 h).

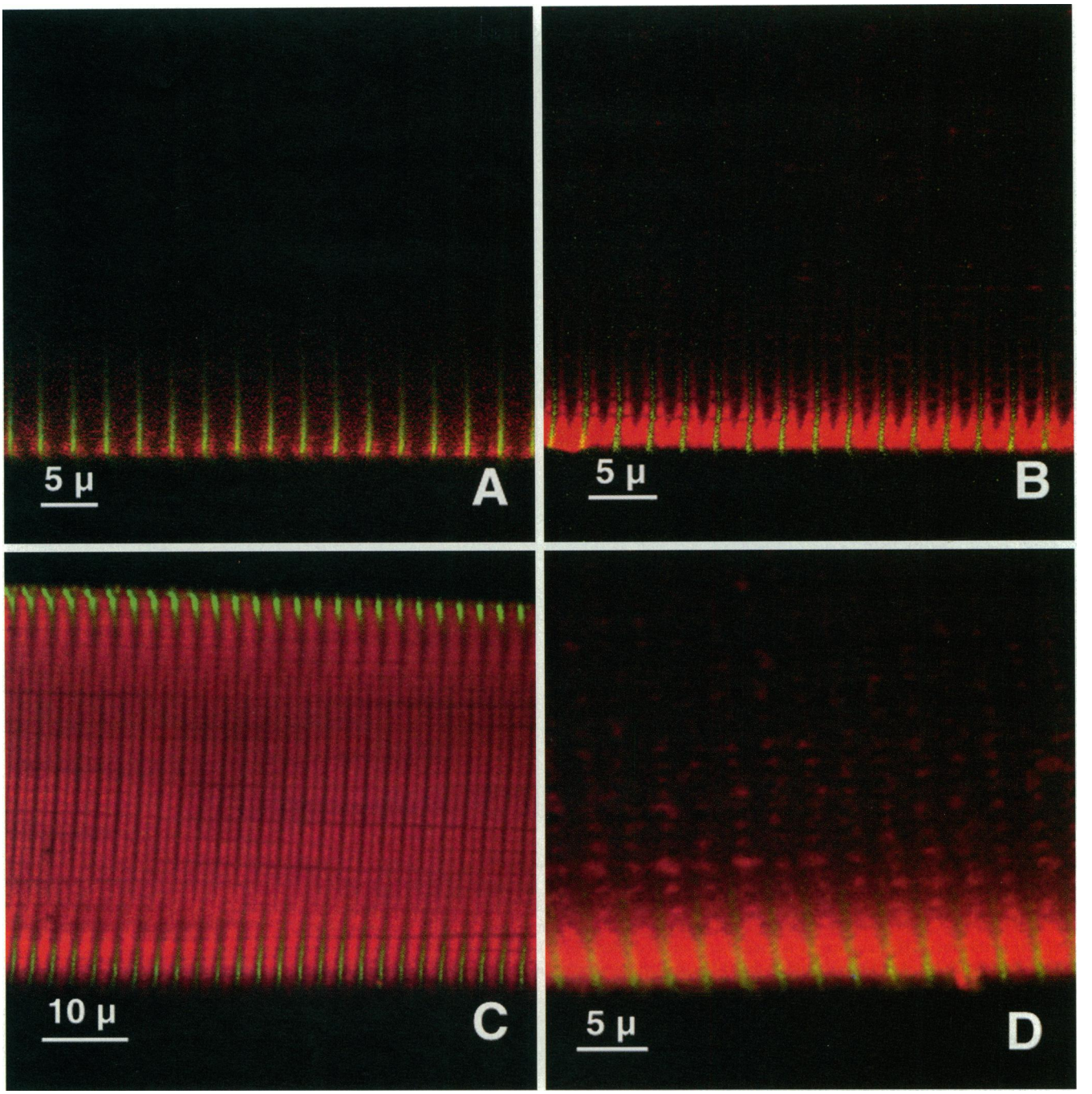

FIGURE 6 Double-fluorescence confocal images of longitudinal optical section through the core of an unfixed skeletal muscle fiber after 2 min (*A*) and 15 min (*B*) of diffusion of 8 μM Rh-NEM-S1 in ATPγS, low [Ca^{2+}]. Both images show only outer layers of one side of the fiber. Center of fiber above upper edge of panels. To identify the M-line, the fiber was preincubated with an anti-myomesin antibody as described in Fig. 5 *B*. The image in *A* was taken with very high gain setting to detect changes in fluorescence intensity at the beginning of diffusion. (*C*) Incubation with 1.7 μM Rh-NEM-S1 for 33 h at low [Ca^{2+}]. Labeling of the M-line as in *A* and *B*. (*D*) Incubation as in *B*, i.e., 15 min, 8 μM Rh-NEM-S1, MgATPγS—however, at high [Ca^{2+}] (pCa 4.5). In *B-D* fluorescence intensity inside the muscle fiber increased above intensity of surrounding solution, indicating accumulation of Rh-NEM-S1 inside the fiber. To prevent saturation of photomultiplier, the gain setting was reduced. (Images are real-time observations of different fibers.)

Rhodamine-labeled muscle creatine-kinase (Rh-MM-CK) also bound preferentially to sites along the M-line (Fig. 5 *C*), where the enzyme was also localized in situ in chemically fixed cryosectioned muscle or in isolated myofibrils (Wegmann et al., 1992). In contrast, the rhodamine-labeled brain-type isoform of creatine-kinase did not bind to the M-line (Rh-BB-CK, Fig. 5 *D*), fully confirming previous results obtained by different means (Wallimann et al., 1983; Schaefer and Perriard, 1988).

Proteins binding in the I-band region of the sarcomere. Diffusion of rhodamine-pyruvate-kinase resulted in an increase of fluorescence intensity in the I-band, indicating

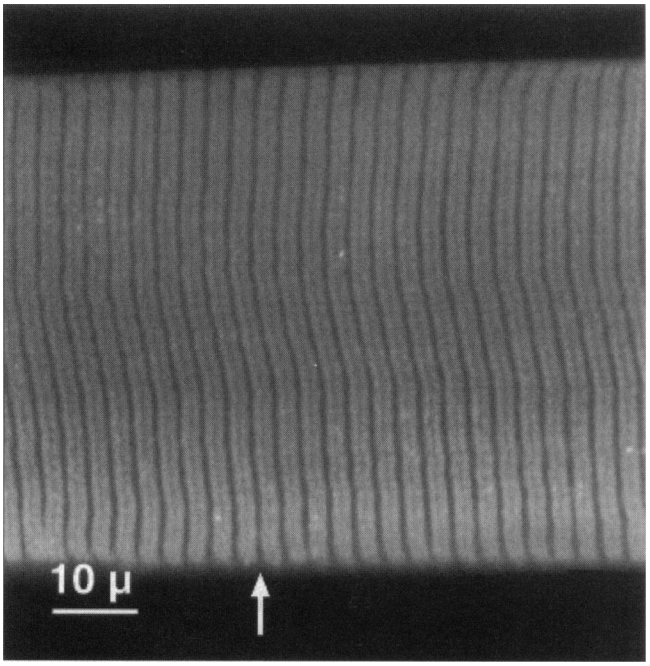

FIGURE 7 Longitudinal optical section through core of a muscle fiber incubated with Rh-NEM-S1 (1.7 μM) for 4 days. Fiber was preincubated for 4 days, followed by fixation before session at confocal microscope.

binding of pyruvate-kinase in this area (Fig. 5 *B*). This is consistent with earlier studies showing that larger complexes of glycolytic enzymes, except for hexokinase, seem to be associated with the actin filament in the I-band (Sigel and Pette, 1969). Although the image was taken after washing out unbound Rh-PK, there still was a low fluorescence intensity also in other parts of the sarcomeres.

At higher recording sensitivity compared with that used for visualization of Rh-MM-CK, a slight increase in fluorescence intensity of the I-band over the background was found after diffusion of Rh-BB-CK into muscle fibers (Fig. 5 *D*) indicating some binding of Rh-BB-CK to this area. This binding, however, seems to be very weak because Rh-BB-CK could be washed out easily.

Time-dependent spatial distribution

Rhodamine-labeled NEM-S1 (Rh-NEM-S1), a modified myosin-subfragment-1 that was shown in solution studies to bind with high affinity to actin, required several days (concentration 1.7 μM) until homogeneous fluorescence labeling was established across the entire fiber (Fig. 7). Because equilibration of Rh-NEM-S1 was rather slow, it was possible to study in detail the time dependence and the progression of the spatial distribution of fluorescent labeling across the muscle fiber and even within the sarcomeres.

Figs. 6 *A-C* and 7 illustrate different stages during diffusion of Rh-NEM-S1 into a muscle fiber under relaxing conditions (pCa 8). MgATPγS was used as an only slowly hydrolysable analog of MgATP to prevent active force generation upon binding of Rh-NEM-S1 to actin. In Fig. 6 *D*, diffusion occurred at high [Ca^{2+}] (pCa 4.5) in the presence of MgATPγS. In Fig. 6, *A*, *B*, and *D*, the center of the fiber is outside the upper edge of each panel. For some of these experiments, higher Rh-NEM-S1 concentrations were used to visualize better the labeling pattern at the very beginning of diffusion. Again, as a standard marker for the M-line of each sarcomere, an antibody against the M-line protein myomesin was used, which was detected by subsequently adding a secondary, FITC-labeled IgG.

Fig. 6 *A* shows the outer layers of the fiber 2 min after the onset of diffusion of 8 μM Rh-NEM-S1 at low [Ca^{2+}]. At this time, the highest fluorescence intensity of Rh-NEM-S1 appeared at the free end of the actin filaments along the H-zone of each sarcomere. As diffusion of Rh-NEM-S1 continued, the high fluorescence spread out toward the core of the fiber but also axially along the actin filaments toward the Z-line of each sarcomere. Fig. 6 *B* shows a picture of the outer layers of a muscle fiber under the same conditions but after 15 min of incubation. Toward the inner layers of the fiber, high fluorescence intensity was found mainly on both sides along the H-zone, indicating large amounts of (bound) Rh-NEM-S1 in the acto-myosin overlap zone. In the outermost layers, where fluorescence labeling has proceeded most toward equilibration within the sarcomeres, high fluorescence intensity was found all along the actin filaments. To distinguish whether the successive labeling of the actin filaments, beginning at their free end at the H-zone, is due to steric hindrance in the diffusion pathway or results from an increase in actin affinity upon binding of Rh-NEM-S1 to the actin filament (activation of the actin filament by Rh-NEM-S1), we followed the time course of fluorescent labeling also at high [Ca^{2+}]. Under these conditions, where the actin filaments are activated even without bound Rh-NEM-S1, binding of Rh-NEM-S1 was homogenous all along the actin filaments from the very beginning of diffusion, i.e., even at low level labeling (Fig. 6 *D*).

Fig. 6 *C* demonstrates that even after several hours of incubation with 1.7 μM Rh-NEM-S1 at low [Ca^{2+}], the fluorescence distribution was still not homogeneous. Only the sarcomeres in the outer layers of the fiber have gained their final staining pattern, whereas there is still an intensity gradient and a different staining pattern toward the center of the fiber. Complete equilibration of a fiber with 1.7 μM Rh-NEM-S1 under relaxing conditions required at least 4 days of incubation. After this time, fluorescence intensity was equally high over the whole cross section of the fiber (Fig. 7).

Because Rh-NEM-S1 binds to actin with high affinity and thus reaches much higher total concentrations (=[free molecules] + [bound molecules]) inside the fiber than outside (=[free molecules]), the resulting fluorescence intensity in these areas is much higher than in the surrounding solution. (Note that to avoid saturation of the photomultiplier, the gain-setting in Figs. 6 *B-D* and 7 had to be reduced compared with Fig. 6 *A*. Therefore, the background in these latter images appears completely black.)

Reversibility of fluorescent labeling

Aside from using confocal microscopy to analyze the time course for equilibration and the spatial distribution and/or redistribution of fluorescent labeling, this method can also be used to assess kinetic properties of binding of fluorescently labeled molecules to their target sites by following the reversibility of fluorescent labeling using an in situ chase protocol.

Reversibility of fluorescent labeling in absence of unlabeled molecules (no chase/exchange)

For molecules like Rh-NEM-S1, Rh-F_{ab}(1–7), or Rh-phalloidine (Fig. 8 *C*), which bind with high affinity to actin, it was impossible to observe a substantial decrease in fluorescence even after several hours of washing with incubation buffer lacking the respective labeled molecule.

In contrast, Rh-123, IgG DaM, and Rh-BB-CK, all molecules that bind only with low affinity to sites within the fiber, disappeared completely from the fiber within a couple of minutes of washing. Rh-MM-CK (Fig. 8, *A* and *B*) was somewhat intermediate in that it required some 8–10 h of washing to observe removal of a significant fraction of the fluorescently labeled enzyme from the M-band.

Reversibility of fluorescent labeling in presence of unlabeled molecules (exchange/chase)

Fig. 8 shows that the time course of the disappearance of Rh-MM-CK from the M-line, while the fiber was kept in a solution without (Fig. 8 *A*, *filled circles*) or with (Fig. 8 *A*, *open triangles*) unlabeled MM-CK. In the presence of unlabeled MM-CK, it took only ~10 min to displace Rh-MM-CK from the M-lines. This suggests that although Rh-MM-CK binds with high affinity to the M-line, as indicated by the slow loss in the absence of unlabeled MM-CK, its rate constant for dissociation apparently is high enough such that it can be replaced rather rapidly by unlabeled enzyme with the displaced material diffusing out of the fiber. The fiber shown in Fig. 8 *A* after equilibration with Rh-MM-CK was not washed to remove Rh-MM-CK bound with low affinity. This may explain the very rapid initial drop in intensity seen after washing both in absence and presence of unlabeled MM-CK (Fig. 8 *A*, *filled circles* and *open triangles*). In the presence of unlabeled MM-CK, the displacement of the material bound with high affinity was so fast that it did not separate from the washout of material bound only with low affinity. Such a rapid initial drop in fluorescence intensity appears typical for MM-CK and is not seen with other molecules like Rh-phalloidine or Rh-troponin and may indicate that part of the Rh-MM-CK is only weakly associated with the M-line.

Similar displacement of fluorescently labeled molecules by unlabeled molecules was also observed with Rh-phalloidine (Fig. 8 *C*) and Rh-troponin (Kraft et al., 1995), except that after a short pre-wash without unlabeled phalloidin (or unlabeled troponin) no rapid initial drop in fluorescence intensity was observed, and that the displacement of fluorescence in presence of unlabeled phalloidin was slower than that in Fig. 8 *A* (decay for troponin is intermediate). This suggests that Rh-phalloidine dissociates somewhat more slowly from actin but the rate that the constant for dissociation is still significant and on a time scale of minutes.

These experiments illustrate the potential of using confocal microscopy to probe in situ the kinetics of dissociation

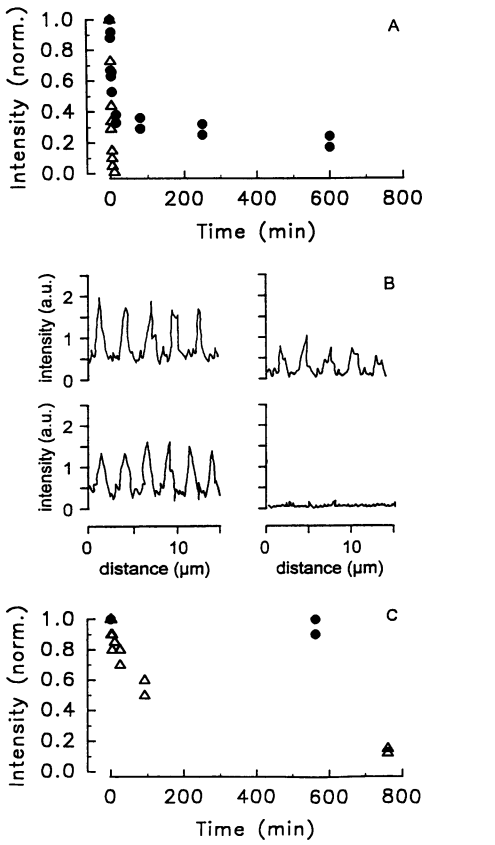

FIGURE 8 (*A*) Time course of the disappearance of Rh-MM-CK from the M-line of a fiber upon incubation in relaxing solution without (●) and with (△) unlabeled MM-CK (4 mg/ml). M-line-associated fluorescence intensity plotted vs. time. Fluorescence intensity normalized with respect to maximum intensity at end of preequilibration with Rh-MM-CK (0.14 mg/ml). Fibers were not preincubated without Rh-MM-CK before recording decay of fluorescence. The rapid initial decrease of M-line fluorescence intensity is characteristic of Rh-MM-CK and may reflect a rapid loss of the fraction of Rh-MM-CK, which is only loosely associated with M-line. Note that in the presence of unlabeled MM-CK, displacement of Rh-MM-CK from the M-line is so fast that it cannot be separated from the period over which the loosely associated material diffuses out of fiber. (*B*) Intensity profiles of fluorescence intensity of Rh-MM-CK parallel to fiber axis. Fluorescence peaks represent Rh-MM-CK bound to M-line of 5–6 sarcomeres. (*top*) Fluorescence intensity before incubation in relaxing solution (*left*) and after 15 min of incubation without unlabeled MM-CK (*right*). (*bottom*) Fluorescence intensity before incubation in relaxing solution (*left*) and after 15 min of incubation with unlabeled MM-CK (*right*). (*C*) Rh-phalloidine (2 μM)-labeled fiber. (●) Fluorescence intensity as a function of time during incubation without unlabeled phalloidin. (△) Decay of fluorescence intensity in presence of unlabeled phalloidin (20 μM).

of fluorescently labeled compounds from their structural binding sites.

DISCUSSION

In the present study, using confocal laser fluorescence microscopy, we were able to visualize the equilibration of several fluorescently labeled molecules within skinned skeletal muscle fibers on a time scale ranging from several minutes to days. The method used does not require chemical fixation of the fibers but, instead, allows observation of equilibration in real time under physiological conditions.

We found that equilibration of molecules that bind with high affinity to sarcomeric sites is slowed down significantly compared with molecules of approximately the same size but without high affinity binding. We could also follow time-dependent changes in characteristic labeling patterns of several substances within the sarcomere that may be used to detect changes in binding affinities that can lead to redistribution of the molecules during equilibration, as well as to estimate in situ the dissociation kinetics of bound molecules.

Estimate of time for equilibration

As described under Materials and Methods, we used longitudinal two-dimensional sections through the core of the fibers to determine equilibration times. However, we did not attempt to fit the time courses of fluorescence changes to a standard diffusion model describing diffusion into a cylinder. Such a mathematical description appears to be inappropriate for the observed equilibration in muscle fibers because, aside from fibers being noncylindrical, several factors obviously complicate the equilibration behavior for some molecules (see below): 1) binding and dissociation of the molecules to/from sites within the sarcomeric structures; 2) changes in pore size as a result of increasing occupancy of binding sites; 3) competition with other molecules for binding sites; and 4) changes in affinities of binding sites on binding (cooperativity effects). As discussed below, the contribution of these factors to the time course of equilibration apparently varies quite extensively from molecule to molecule and, thus, results in the unexpectedly large variations in equilibration times for the different molecules described in this paper. Thus, even with a complete mathematical model accounting for these factors, it would be impossible to estimate equilibration times for various molecules from the known time course of only a few examples without detailed knowledge of the contribution made by other factors affecting equilibration for each individual system. Because it was our main goal to develop an approach to determine the incubation times that are necessary for equilibration of molecules that are diffused into muscle fibers for physiological studies, it appeared to us quite misleading to approximate such a time course by a generalized model implying usefulness for extrapolation of equilibration times for other molecules. Rather, we emphasize that for each individual case equilibration times should be determined experimentally.

Factors limiting equilibration

Studying the efflux of cytosolic muscle proteins out of skinned fibers, Maughan and Lord (1985) found that diffusion of these molecules was reduced by a factor of 10–50 relative to their diffusivity in aqueous solution. In contrast to our observations (Fig. 3), they found an inverse correlation between molecular weight and diffusion coefficient. Because of the short observation time of 1 h and the applied method (following the efflux of molecules out of the fiber), they may have examined only the efflux of molecules that move rather easily through the cytoplasm and that bind, if at all, only with low affinity to cellular structures. For such molecules, it is quite possible that, as Maughan and Lord (1985) proposed, molecular weight, tortuosity, and viscosity are the major rate-limiting factors for efflux out of skinned fibers. In our study, because of the dead-time of solution exchange, we could not detect reliably differences in equilibration time for rapidly equilibrating (<2–3 min) molecules even though they differed greatly in their molecular weights, e.g., TxR-DaM-IgG and Rh-123. The missing correlation between time for equilibration and molecular weight for slowly equilibrating molecules in our study (Fig. 3) suggests that other factors than molecular weight dominate the time required for their equilibration.

The large gradient in fluorescence intensity across the fiber from the beginning of diffusion until equilibrium is reached (e.g., Rh-NEM-S1, Fig. 6) shows that 1) slow equilibration is not due to a diffusion barrier at the fiber surface and 2) that binding of the molecules to sarcomeric structures is fast on the time scale of diffusion, as it was assumed by Gershon et al. (1985). Both slow binding with high mobility and a diffusion barrier at the fiber surface should result theoretically in a slow but homogeneous increase in fluorescence intensity across the whole fiber.

The very large increase in fluorescence intensity inside the fibers above background intensity during equilibration, seen with several different molecules, and resulting in a specific binding pattern (e.g., TRITC-anti-actin-IgG, TRITC-F_{ab}(1–7), and Rh-NEM-S1), indicates binding of these molecules to a large number of specific sites. This phenomenon often corresponded to very long equilibration times. Apparently, even if the mobility of the molecules were unchanged during the process of equilibration, loading of the fiber and, thus, equilibration take much longer if many sites inside the fiber have to be saturated (e.g., TRITC-anti-actin-IgG) compared with molecules of identical mobility but with little binding to sarcomeric structures (e.g., TxR-DaM-IgG, Fig. 4). Successive recruitment of molecules from the surrounding solution might explain, at least in part, the slow equilibration of such molecules.

In addition, in muscle fibers, large molecules might also be retarded during equilibration because of limited pore size

within the cytoplasmic matrix (molecular sieve). This holds especially true for the actomyosin overlap zone, which is heavily populated by cross-bridges with little void volume left, acting as a molecular sieve, especially in rigor when cross-bridges are bound to actin (Wegmann et al., 1992). Gershon et al. (1985) determined 100 nm as pore size in a PTK cell, and the diffusing molecules in their study were smaller than that. Thus, no significant limitation of equilibration by pore size was expected for the system they studied. In a muscle fiber, however, the size of the free space between the contractile proteins and cytoskeletal structures presumably is smaller (~10–20 nm, Wegmann et al., 1992). Also, binding of molecules to sarcomeric structures might cause an additional obstruction by further reducing the pore size. On this basis, differences and changes in accessibility of interfilament space might contribute, for example, to the very large difference in equilibration time for Rh-phalloidine compared with TRITC-F_{ab}(1–7), TRITC-anti-actin-IgG, and Rh-NEM-S1, all of which are expected to bind to actin with high affinity and 1:1 stoichiometry (same number of sites to be saturated).

Furthermore, based on experiments by Wojcieszyn et al. (1981), showing that proteins move much more slowly through the cytoplasmic matrix than in water, Gershon and co-workers (1985) proposed that diffusional motion of proteins can be slowed down significantly by binding and dissociation of the proteins to and from the cytoplasmic matrix. In their diffusion-adsorption model, the diffusing molecules are thought to bind instantaneously to cellular structures and that this interaction is much faster than diffusion. Furthermore, the binding constants that Gershon et al. (1985) derived for several proteins indicate that at any given time most molecules are bound to the cytomatrix, although the rates of association and dissociation might be quite high.

Finally, equilibration could also be affected by competition of the molecules for binding sites or exchange with bound native proteins. For example, it was discussed that binding of Rh-phalloidine is affected by the presence of nebulin along the actin filament (Ao and Lehrer, 1995). Alternatively, Rh-MM-CK is a molecule for which equilibration might be affected by exchange with native MM-CK in the muscle fibers. To probe whether fibers retain some of their native M-line associated MM-CK during chemical skinning with Triton-X-100, we followed the time course of binding of Rh-MM-CK to the M-line after the fiber had been preincubated with unlabeled MM-CK. Equilibration of fibers with Rh-MM-CK was slowed down when fibers were preincubated with unlabeled MM-CK most likely because Rh-MM-CK had to replace bound MM-CK, whereas in untreated skinned fibers at least some of the sites are unoccupied.

It should be noted that in all cases equilibration could be accelerated by using higher concentrations of the diffusing molecules which, of course, causes a higher concentration gradient and, therefore, faster diffusion. After equilibration, this would also cause, however, a higher occupancy of the binding sites with the particular molecule. On the other hand, for many experiments, e.g., mechanical experiments with muscle fibers loaded with Rh-NEM-S1, only a partial occupancy yet homogeneous distribution is required, which can only be achieved by using lower concentrations of the diffusing molecule but, consequently, very much longer diffusion times are needed. One might also argue that for the diffusion of fluorescently labeled antibodies much higher concentrations could be used. This, however, is likely to cause nonspecific binding to other epitopes and, therefore, to give misleading staining patterns.

Binding patterns and entry pathways

For several molecules, after equilibration the fluorescence intensity inside the fiber was very much larger than in the incubation medium surrounding the fiber, indicating extensive binding to sarcomeric structures. Whenever such binding occurred to specific sites, fluorescence labeling patterns were found that are characteristic for the respective compound.

For slowly equilibrating compounds, however, not only a characteristic labeling pattern could be observed after equilibration, but also the development of such labeling patterns with time could be resolved. Such a detailed study was possible with Rh-NEM-S1. Comparison with equilibration in the presence of calcium suggests that the nonuniform increase in fluorescence intensity along the actin filaments is not the result of unequal accessibility of the sarcomeres for Rh-NEM-S1 but, instead, reflects a gradual increase in affinity of actin for Rh-NEM-S1 upon its binding. Because of cooperativity along the actin filaments, activation by bound Rh-NEM-S1 facilitates binding of Rh-NEM-S1 to regions next to the activated part of the filaments. Fluorescence intensity increasing from the free end of the actin filaments indicates that the filaments are activated most easily at this free end, possibly because the regulated unit (7 actin-monomers + troponin + tropomyosin) at the free end of the actin filament is in contact with only one nonactivated nearest-neighbor unit. Because fluorescence proceeded only gradually from the free end toward the Z-line, cooperativity along the actin filament appears to extend only over a few regulated actin units, i.e., activation of only a few regulated units apparently is not sufficient to activate the thin filament as a whole. Similar limited cooperativity was suggested by Swartz et al. (1990) when studying binding of S1 in myofibrils under rigor conditions.

Reversibility of fluorescent labeling: extraction versus exchange of sarcomeric proteins

Following the reversibility of fluorescent labeling, we found that molecules that bind with high affinity within the fibers are released only slowly or not at all from the fibers (Rh-phalloidine, Rh-troponin). They may be released readily, however, through exchange for unlabeled homologous mol-

ecules without changes in buffer conditions (e.g., pH, ionic strength, etc.) to reduce affinities for their sarcomeric binding sites. The speed of such displacement is expected to depend on the rate of dissociation of the fluorescent molecule from its binding site (e.g., Rh-phalloidine vs. Rh-MM-CK in Fig. 8). Apparently, once a fluorescently labeled molecule has dissociated from its binding site, it is replaced quickly by an unlabeled molecule (concentration of unlabeled compound $\gg$ free concentration of labeled compound). The dissociated molecule is free to diffuse out of the fiber because at high concentration of the unlabeled compound essentially all binding sites are saturated such that the probability for the fluorescent molecule to rebind anywhere is very low. In the absence of the unlabeled compound, a fluorescently labeled molecule, once dissociated from its binding site, would rebind rapidly to this or any other unoccupied site and diffusion out of fiber would be very much slowed down, unless the affinity for free binding sites is reduced drastically by changes in experimental conditions.

In conclusion, our observations support the view that in structured systems one is not dealing with "simple" diffusion but, instead, with a complex process of equilibration. It appears to be affected strongly by interactions of the moving molecules with structural proteins including additional obstruction effects upon binding, time required for saturation of many binding sites, competition of the molecules for binding sites, or exchange with native proteins. Together with the noncylindrical cross section of the fibers, we consider it inappropriate to describe the time course of equilibration as standard diffusion and to fit the data to such a model. The observed exchange even for molecules that bind with very high affinity to sites along the myofilaments illustrates the potential of using chase protocols for exchanging sarcomeric proteins for fluorescently labeled isoforms or modified molecules.

This work was supported by SNF grant 31-33907.92 and a grant of the Swiss Society for Muscle Diseases, both given to T.W. and by a DFG grant given to B.B. (Br849/1-4).

REFERENCES

Ao, X., and S. S. Lehrer. 1994. Observations of the kinetics of rhodamine phalloidin binding to actin in rabbit skeletal and cardiac myofibrils. *Biophys. J.* 66:194*a*. (Abstr.)

Ashizawa, K., P. McPhie, K.-H. Lin, and S.-Y. Cheng. 1991. An in vitro novel mechanism of regulating the activity of pyruvate kinase M_2 by thyroid hormone and fructose 1,6-bisphosphate. *Biochemistry*. 30: 7107–7111.

Brenner, B. 1993. Technique for stabilizing the striation pattern in maximally calcium-activated skinned rabbit psoas fibers. *Biophys. J.* 41: 99–102.

DasGupta, G., and E. Reisler. 1992. Actomyosin interactions in the presence of ATP and the N-terminal segment of actin. *Biochemistry*. 31: 1836–1841.

Edidin, M., Y. Zagyanski, and T. J. Lardner. 1976. Measurement of membrane protein lateral diffusion in single cells. *Science*. 191: 466–468.

Engel, J., M. Fechner, A. J. Sowerby, S. A. W. Finch, and A. Stier. 1994. Anisotropic propagation of calcium waves in isolated cardiomyocytes. *Biophys. J.* 66:1756–1762.

Eppenberger, H. M., J. C. Perriard, U. B. Rosenberg, and E. E. Strehler. 1981. The M_r 165,000 M-protein myomesin. A specific protein of cross-striated muscle cells. *J. Cell. Biol.* 89:185–193.

Gershon, N. D., K. R. Porter, and B. L. Trus. 1985. The cytoplasmic matrix: its volume and surface area and the diffusion of molecules through it. *Proc. Natl. Acad. Sci. USA*. 82:5030–5034.

Grove, B. K., V. Kurer, Ch. Lehner, T. C. Doetschman, J. C. Perriard, and H. M. Eppenberger. 1984. A new 185,000-dalton skeletal muscle protein detected by monoclonal antibodies. *J. Cell Biol.* 98:518–524.

Hill, A. V. 1948. On the time required for diffusion and its relation to processes in muscle. *Proc. R. Soc. Lond. Ser. B*. 135:446–453.

Hofer, H. W., G. Gerlach, G. Birkel, and H. L. Kirschenlohr. 1987. The possible significance of interactions between soluble proteins in skeletal muscle. *Biochem. Soc. Trans.* 15:982–985.

Horowitz, S. B., and L. C. Moore. 1974. The nuclear permeability, intracellular distribution, and diffusion of inulin in the amphibian oocyte. *J. Cell Biol.* 54:609–625.

Jacobson, K., and J. Wojcieszyn. 1984. The translational mobility of substances within the cytoplasmic matrix. *Proc. Natl. Acad. Sci. USA*. 81:6747–6751.

Jones, D. A., and J. M. Round. 1990. Skeletal Muscle in Health and Disease. Manchester University Press, Manchester, U.K.

Keleti, T. 1990. Control of Metabolic Processes. A. Cornish-Bowden and M. L. Cardenas, editors. Plenum Press, New York. 259–270.

Kraft, T., M. Messerli, B. Rothen-Rutishauser, T. Wallimann, J.-C. Perriard, J. M. Chalovich, and B. Brenner. 1995. Equilibration and exchange of fluoescently labeled molecules in skeletal muscle fibers studied using confocal microscopy. *Biophys. J.* 68:371*a*. (Abstr.)

Kraft, T., J. M. Chalovich, L. C. Yu, and B. Brenner. 1995. Parallel inhibition of active force and relaxed fiber stiffness by caldesmon at near physiological conditions. Further evidence that weak cross-bridge binding to actin is an essential intermediate for force generation. *Biophys. J.* 68:2404–2418.

Kraft, T., M. Messerli, B. Rutishauser, J. C. Perriard, T. Wallimann, and B. Brenner. 1993. Diffusion of fluorescently labeled proteins into skinned skeletal muscle fibers observed by confocal microscopy. *Biophys. J.* 64:26*a*. (Abstr.)

Kurganov B. I., N. P. Ssugrobava, and L. S. Milman. 1985. Supramolecular organization of glycolytic enzymes. *J. Theor. Biol.* 116:509–526.

Kushmerick, M. J., and R. J. Podolsky. 1969. Ionic mobility in muscle cells. *Science* 166:1297–1298.

Mastro, A. M., M. A. Babich, W. D. Taylor, and A. D. Keith. 1984. Diffusion of a small molecule in the cytoplasm of mammalian cells. *Proc. Natl. Acad. Sci. USA*. 81:3414–3418.

Maughan, D., and C. Lord. 1988. Protein diffusivities in skinned frog skeletal muscle fibers. *Adv. Exp. Med. Biol.* 226:75–84.

Messerli, J. M., H. T. M. van der Voort, E. Rungger-Braendle, and J.-C. Perriard. 1993. Three-dimensional visualization of multi-channel volume data: the amSFP algorithm. *Cytometry*. 14:725–735.

Minsky, M. 1957. Microscopy Apparatus. U.S. patent 3013467.

Nicholson, C., and L. Tao. 1993. Hindered diffusion of high molecular weight compounds in brain extracellular microenvironment measured with integrative optical imaging. *Biophys. J.* 65:2277–2290.

Olson, A., and E. N. Pugh. 1993. Diffusion coefficient of cyclic GMP in salamander rod outer segments estimated with two fluorescent probes. *Biophys. J.* 65:1335–1352.

Ono, T., K. Ono, K. Mizukawa, T. Ohta, T. Tsuchiya, and M. Tsuda. 1994. Limited diffusibility of gene products directed by a single nucleus in the cytoplasm of multinucleated myofibers. *FEBS Lett.* 337:18–22.

Paine, P. L., L. C. Moore, and S. B. Horowitz. 1975. Nuclear envelope permeability. *Nature*. 254:109–114.

Saks, V. A., and Ventura-Clapier, R. 1992. Biochemical organization of energy metabolism in muscle. *J. Biochem. Org*. 1:9–29.

Schaefer, B. W., and J. C. Perriard. 1988. Intracellular targeting of isoproteins in muscle cytoarchitecture. *J. Cell Biol.* 106:1161–1170.

Schnekenbühl, S., T. Kraft, L. C. Yu, B. Brenner, and J. M. Chalovich. 1992. Effect of NEM-S1 on cross-bridge action in skinned rabbit psoas muscle fibers. Biochemical, mechanical and X-ray diffraction studies. *Biophys. J.* 61:292*a*. (Abstr.)

Sheppard, C. J. R. 1987. Scanning Optical Microscopy 10. Academic Press, London.

Sigel, P., and D. Pette. 1969. Intracellular localisation of glycogenolytic and glycolytic enzymes in white and red rabbit skeletal muscle. *J. Histochem. Cytochem.* 17:225–237.

Swartz, D. R., M. L. Greaser, and B. B. Marsh. 1990. Regulation of binding of subfragment 1 in isolated rigor myofibrils. *J. Cell. Biol.* 111: 2989–3001.

Wallimann, T., H. Moser, and H. M. Eppenberger. 1983. Isoenzyme-specific localisation of M-line bound creatine kinase in myogenic cells. *J. Muscle Res. Cell Motil.* 4:429–441.

Weeds, A. G., and R. S. Taylor. 1975. Separation of subfragment-1 isoenzymes from rabbit skeletal muscle myosin. *Nature.* 257:54–56.

Wegmann, E., E. Zanolla, H. M. Eppenberger, and Wallimann, T. 1992. In situ compartimentation of creatine kinase in intact sarcomeric muscle: the acto-myosin overlap zone as a molecular sieve. *J. Muscle Res. Cell Motil.* 13:420–435.

Williams, D. L., L. E. Greene, and E. Eisenberg. 1984. Comparison of effects of smooth and skeletal tropomyosins on interactions of actin and myosin subfragment 1. *Biochemistry.* 23:4150–4155.

Wojcieszyn, J. W., R. A. Schlegel, E.-S. Wu, and K. A. Jacobson. 1981. Diffusion of injected macromolecules within the cytoplasm of living cells. *Proc. Natl. Acad. Sci. USA.* 78:4407–4410.

Yu, L. C., and B. Brenner. 1989. Structures of actomyosin cross-bridges in relaxed and rigor muscle fibers. *Biophys. J.* 55:441–453.